eISSN 2005-5447
International Journal of Stem Cells Vol. 18, No. 2, 2025 https://doi.org/10.15283/ijsc25011

BRIEF REPORT

Loss of Ubiquitin-Specific Protease 11 Mitigates Pulmonary Fibrosis in Human Pluripotent Stem Cell-Derived Alveolar Organoids

Sripriya Rajkumar[1,*], Ji-Hye Jung[2,*], Ji-Young Kim[2,*], Janardhan Keshav Karapurkar[1], Girish Birappa[1], D. A. Ayush Gowda[1], C. Bindu Ajaykumar[1], Haribalan Perumalsamy[3], Bharathi Suresh[1], Kye-Seong Kim[1,4], Seok-Ho Hong[2,5], Suresh Ramakrishna[1,4]

[1]*Graduate School of Biomedical Science and Engineering, Hanyang University, Seoul, Korea*
[2]*Department of Internal Medicine, College of Medicine, Kangwon National University, Chuncheon, Korea*
[3]*Research Institute for Convergence of Basic Science, Hanyang University, Seoul, Korea*
[4]*College of Medicine, Hanyang University, Seoul, Korea*
[5]*KW-Bio Co., Ltd, Chuncheon, Korea*

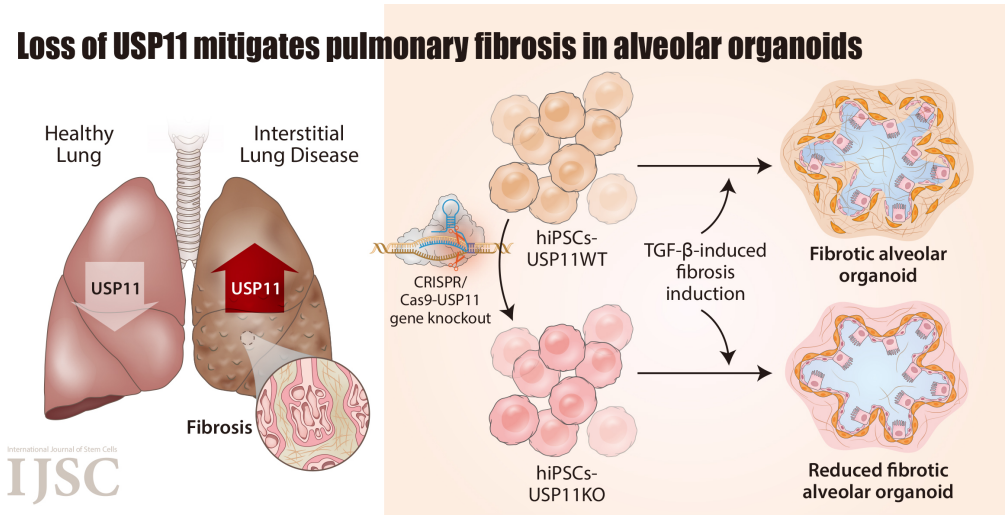

Received: February 18, 2025, Revised: March 17, 2025, Accepted: March 17, 2025, Published online: April 7, 2025
Correspondence to **Suresh Ramakrishna**
Graduate School of Biomedical Science and Engineering, Hanyang University, 222 Wangsimni-ro, Seongdong-gu, Seoul 04763, Korea
E-mail: suri28@hanyang.ac.kr
Co-Correspondence to **Seok-Ho Hong**
Department of Internal Medicine, College of Medicine, Kangwon National University, 1 Kangwondaehak-gil, Chuncheon 24341, Korea
E-mail: shhong@kangwon.ac.kr
Co-Correspondence to **Kye-Seong Kim**
Graduate School of Biomedical Science and Engineering, Hanyang University, 222 Wangsimni-ro, Seongdong-gu, Seoul 04763, Korea
E-mail: ks66kim@hanyang.ac.kr
*These authors contributed equally to this work.

Loss of Ubiquitin-Specific Protease 11 Mitigates Pulmonary Fibrosis in Human Pluripotent Stem Cell-Derived Alveolar Organoids

Sripriya Rajkumar[1,*], Ji-Hye Jung[2,*], Ji-Young Kim[2,*], Janardhan Keshav Karapurkar[1], Girish Birappa[1], D. A. Ayush Gowda[1], C. Bindu Ajaykumar[1], Haribalan Perumalsamy[3], Bharathi Suresh[1], Kye-Seong Kim[1,4], Seok-Ho Hong[2,5], Suresh Ramakrishna[1,4]

[1]*Graduate School of Biomedical Science and Engineering, Hanyang University, Seoul, Korea*
[2]*Department of Internal Medicine, College of Medicine, Kangwon National University, Chuncheon, Korea*
[3]*Research Institute for Convergence of Basic Science, Hanyang University, Seoul, Korea*
[4]*College of Medicine, Hanyang University, Seoul, Korea*
[5]*KW-Bio Co., Ltd, Chuncheon, Korea*

The etiology of chronic and lethal interstitial lung disease, termed idiopathic pulmonary fibrosis (IPF), remains unidentified. IPF induces pathological lung scarring that results in rigidity and impairs gas exchange, eventually resulting in premature mortality. Recent findings indicate that deubiquitinating enzymes play a key role in stabilizing fibrotic proteins and contribute to pulmonary fibrosis. The ubiquitin-specific protease 11 (USP11) promotes pro-fibrotic proteins, and its expression elevated in tissue samples from patients with IPF. Thus, this study aimed to examine the effects of loss of function of *USP11* gene on the progression of pulmonary fibrosis by utilizing 3D cell culture alveolar organoids (AOs) that replicate the structure and functions of the proximal and distal airways and alveoli. Here, we applied the CRISPR/Cas9 system to knock out the *USP11* gene in human induced pluripotent stem cells (hiPSCs) and then differentiated these hiPSCs into AOs. Loss of *USP11* gene resulted in abnormalities in type 2 alveolar epithelial cells in the hiPSC-USP11KO-AOs. Moreover, knock out of the *USP11* mitigates pulmonary fibrosis caused by TGF-β in hiPSC-USP11KO-AOs by reducing collagen formation and fibrotic markers, suggesting it has the therapeutic potential to treat IPF patients.

Keywords: Alveolar organoid, Deubiquitinating enzymes, USP11, Pulmonary fibrosis, Loss of function

Introduction

Interstitial lung disease encompasses a diverse range of chronic pulmonary disorders characterized by varying degrees of inflammation and fibrosis. Idiopathic pulmonary fibrosis (IPF) is a chronic, progressive fibrotic disorder of

Received: February 18, 2025, Revised: March 17, 2025, Accepted: March 17, 2025, Published online: April 7, 2025
Correspondence to **Suresh Ramakrishna**
Graduate School of Biomedical Science and Engineering, Hanyang University, 222 Wangsimni-ro, Seongdong-gu, Seoul 04763, Korea
E-mail: suri28@hanyang.ac.kr
Co-Correspondence to **Seok-Ho Hong**
Department of Internal Medicine, College of Medicine, Kangwon National University, 1 Kangwondaehak-gil, Chuncheon 24341, Korea
E-mail: shhong@kangwon.ac.kr
Co-Correspondence to **Kye-Seong Kim**
Graduate School of Biomedical Science and Engineering, Hanyang University, 222 Wangsimni-ro, Seongdong-gu, Seoul 04763, Korea
E-mail: ks66kim@hanyang.ac.kr
*These authors contributed equally to this work.

unknown etiology that results in lung scarring, impaired gas exchange, and accumulation of extracellular matrix proteins. Ultimately, this leads to respiratory failure, with death typically occurring within 3 to 4 years post-diagnosis. The progression of IPF is marked by fibroblast activation and differentiation, recurrent lung injury, excessive cytokine release, and the epithelial–mesenchymal transition (EMT). The biological mechanisms governing the interactions between fibroblasts and epithelial cells, as well as their role in IPF progression, remain unclear, emphasizing the importance of investigating novel and efficacious alternative therapies (1-4).

Ubiquitination and deubiquitination are two essential process within the ubiquitin-proteasome system (UPS) of cell. Any aberration in the balance between these two processes in the lungs results in activation of various intracellular mechanisms including the EMT and cytokine production (5). Deubiquitinating enzymes (DUBs) are proteases that modulate protein degradation by cleaving ubiquitin moieties from diverse protein substrates, promoting protein homeostasis and recycling free ubiquitin molecules for the UPS. DUBs are classified into seven families based on their catalytic and ubiquitin-protease domains (6). The ubiquitin-specific protease (USP) family is the largest and most extensively studied group. Importantly, USP11 belongs to the USP family of proteins, which deubiquitinates and stabilizes the profibrotic protein GREM1 and promotes IPF (7). Moreover, the expression of USP11 is elevated in human IPF patient samples (8), suggesting it as a major therapeutic target for IPF.

In this study, we aimed to examine the role of USP11 in the progression of pulmonary fibrosis (PF) using alveolar organoids (AOs) derived from human induced pluripotent stem cells (hiPSCs). Human organoids simulate the structures and functions of the proximal and distal airways and alveoli, enabling investigation of fibrotic changes. We conducted CRISPR/Cas9-mediated knockout of *USP11* gene in hiPSCs and differentiated these hiPSCs into AOs to investigate the role of USP11 in PF.

Materials and Methods

Cell culture

hiPSCs (Cat. No. A18943PIS; Gibco) were maintained on BD Matrigel (Cat. No. 356230; BD Biosciences)-coated dishes in StemFlex™ Medium (Cat. no. A3349401; Gibco) supplemented with 10 μM Y-27632 dihydrochloride (Cat. No. 1254; Tocris). Before being used in experiments, all cell lines were treated with Plasmocin mycoplasma eliminating reagent (Cat. No. ant-mpt-1; InvivoGen) according to the manufacturer's instructions. Mycoplasma contamination was tested using a MycoAlert Mycoplasma Detection Kit (Cat. No. LT07-118; Lonza Bioscience).

Plasmids, sgRNAs

pCAG-Cas9-GFP (#44719) plasmids were purchased from Addgene. Briefly, oligonucleotides with the *USP11* target sequence were synthesized (Bioneer), and T4 polynucleotide kinase was used to add terminal phosphates to the annealed oligonucleotides (Bio-Rad). The vector was digested using the *BsaI* restriction enzyme and ligated with the annealed oligonucleotides. The target sequences for the sgRNAs targeting *USP11* are listed in Supplementary Table S1 respectively.

Antibodies and reagents

Mouse monoclonal antibodies against GAPDH (1 : 1,000, sc-32233), USP11 (1 : 1,000, sc-365528), COL1A1 (1 : 500, sc-293182), vimentin (1 : 700, ab8978; Abcam), alpha-smooth muscle actin (α-SMA, 1 : 500, sc-53015), and normal mouse IgG (1 : 1,000, sc-2025) were purchased from Santa Cruz Biotechnology. Rabbit polyclonal antibodies against OCT3/4 (1 : 500, ab18976; Abcam), SOX2 (1 : 250, sc-365823; Santa Cruz Biotechnology), SSEA4 (1 : 250, 90231; Millipore), and 488/594-conjugated secondary antibodies (Cat. no. A21207, A21203, 1 : 200; Life Technologies) were used.

Protein 5X sample buffer (Cat. no. EBA-1052; Elpis Biotech), protease inhibitor cocktail (Cat. no. 11836153001; Roche), puromycin (Cat. no. 12122530; Gibco), Recombinant Human TGF-beta 1 protein (Cat. no. 240-B; Bio-Techne), and 4',6-diamidino-2-phenylindole (DAPI, Cat. no. H-1200; VectorLabs) were purchased and used.

T7 endonuclease 1 assay

Genomic DNA was isolated using DNeasy Blood & Tissue Kits (Promega) according to the manufacturer's protocols. The region of DNA containing the sgRNA target site was amplified by polymerase chain reaction (PCR) and denatured and annealed by stepwise heating to form heteroduplex DNA. The heteroduplex DNA was then treated with 5 units of T7 endonuclease 1 (T7E1; New England Biolabs) for 15 to 20 minutes at 37℃, followed by 2% agarose gel electrophoresis. The band intensity was quantified using ImageJ software (National Institutes of Health), and mutation frequencies were calculated using the following equation:

$$\text{Mutation frequency (\%)} = 100 \times [1 - (1 - \text{fraction cleaved})1/2],$$

where the fraction cleaved was the total relative density

of the cleavage bands divided by the sum of the relative density of the cleaved and uncut bands. The oligonucleotide sequences used for PCR amplification and the PCR-amplicon sizes of the *USP11* genes and expected cleavage size after the T7E1 assay are summarized in Supplementary Table S2 and S3, respectively.

Immunofluorescence staining

The cells were grown on glass coverslips and incubated at 37℃ in a humidified atmosphere with 5% CO_2. The cells were washed with phosphate-buffered saline (PBS; Gibco), fixed for 15 minutes using 4% paraformaldehyde (PFA; Biosesang), and permeabilized in PBS containing 0.1% Triton X for 5 minutes at room temperature (RT). The cells were washed, blocked in 3% bovine serum albumin, and stained with the indicated primary antibodies overnight at 4℃. The next day, the cells were washed with PBS and incubated with Alexa Fluor 488–conjugated secondary antibodies for 1 hour. The nuclei were stained with DAPI, and the cells were mounted using VectaShield (VectorLabs). The cells were then visualized, and images were produced using a Leica fluorescence microscope (DM 5000B, CTR 5000; Leica Microsystems).

Generation of the *USP11-KO* in hiPSCs using CRISPR/Cas9

The hiPSCs were co-transfected with a plasmid encoding pCAG-Cas9-GFP, sgRNA targeting *USP11* or non-sgRNA (mock control) using Lipofectamine stem transfection reagent (STEM00001; Thermo Fisher Scientific), according to the manufacturer's instructions. Later, cells expressing GFP were sorted using flow cytometry. The sorted cells were treated with rock inhibitor (10 μmol/mL) and seeded into 96-well plates and incubated in a CO_2 incubator at 37℃. After 15 days, the wells were microscopically evaluated, and the single cell–derived colonies were selected. The selected colonies were dissociated using gentle cell dissociation reagent (Cat. No. 100-0485; Stem Cell Technologies) and reseeded into 24-well cell culture plates. A small portion of the cells was screened for *USP11* gene disruption by the T7E1 assay. The hiPSCs-USP11KO single cell–derived clones were expanded and stored in a liquid nitrogen tank.

Alkaline phosphatase staining

Alkaline phosphatase staining (ALP) was performed according to the manufacturer's protocol. Briefly hiPSCs were cultured for 5 days and cells were washed with PBS and fixed in 4% PFA for 15 minutes and then the cells were stained using ALP detection kit (Cat. no. 86R-1KT; Sigma-Aldrich). The staining solution was added and the cells were incubated in the dark for 1 hour and post incubation the cells were washed twice with TBST and colonies were examined for the appearance of red pink/red coloration. The stained colonies were imaged using microscope (IX71; Olympus).

Stepwise differentiation of hiPSCs into alveolar epithelial cells

Stepwise direct alveolar epithelial cell (AEC) differentiation was performed as previously described (9-11). Briefly, undifferentiated hiPSCs were mechanically passed and then plated in dishes coated with matrigel at a density of 8～10 colonies. After 4～5 days, AEC differentiation was initiated through exposure to stepwise induction media.

Magnetic-activated cell sorting and the generation of AOs from hiPSCs

AOs were generated using a combination of previously reported protocols with minor modifications (9-11). Briefly, the AEC cultures were dissociated with 0.8 U/mL collagenase B (Roche) for 1 hour in a 37℃ incubator on day 21 of AEC differentiation, followed by treatment with cell dissociation buffer (Gibco) for 10 minutes in a 37℃ water bath. The single cell suspension was blended with 20 μL of anti-human CD326 IgG microbeads (EpCAM; Miltenyi Biotec) and then incubated at 4℃ for 30 minutes. After two washes, the labeled cells were applied to an LS column (Miltenyi Biotec), and the magnetically labeled EPCAM-positive cells were eluted. Last, a flow cytometry analysis was conducted to determine the purity of the isolated AECs. The EpCAM-positive cells were seeded into 96-well round-bottom plates (2.5×10^4 cells per well; Corning) containing AEC maturation medium. After distribution, 1 : 15 diluted Matrigel (50 μL per well) was added to each well to improve adhesion between cells, and the plates were incubated overnight at 37℃ in a humidified atmosphere with 5% CO_2 to allow aggregation. After the overnight incubation, the aggregates were transferred to 6-well low-attachment plates (Corning) containing fresh AEC maturation medium and cultured for 9 days to establish AOs. To induce PF in AOs, we used fibrosis inducer transforming growth factor (TGF)-β at an optimized concentration of 25 ng/mL for 72 hours.

Immunohistochemistry of paraffin sections

Formalin-fixed paraffin-embedded hiPSC-USP11WT-AOs and hiPSC-USP11KO-AOs were deparaffinized using xylene and alcohol gradient and slides were blocked for endogenous peroxidase activity by treatment with DAKO

Real Peroxidase Blocking Solution for 40 minutes at RT. After being blocked with serum-free, liquid protein block (X0909; Agilent), the slides were incubated with primary antibodies overnight at 4℃. The slides were washed in PBS with 0.1% Tween, and fluorescently conjugated secondary antibodies were applied for 1 hour at RT in the dark. After washing, the slides were covered with Fluoroshield™ (ab64230; Abcam) mounting medium containing DAPI and photographed using a fluorescence microscope (Olympus). Samples from at least three AOs were used in each group, and data were obtained from 3～5 fields per sample.

Quantitative real-time reverse transcription-PCR

For AOs total RNA was extracted using the RNeasy Mini kit (Qiagen), and cDNA was synthesized using TOPscript™ RT DryMIX (Enzynomics). PCR amplification was performed using a StepOnePlus Real-Time PCR System (Applied Biosystems) and TOPreal™ qPCR 2X PreMIX (Enzynomics). All mRNA expression was normalized to an internal control, GAPDH. The expression levels of the target gene mRNAs were calculated by comparing them to the expression levels of GAPDH using the $2^{-\Delta\Delta Ct}$ method. Primer sequences for human are shown in Supplementary Table S4.

Histological examination

Paraffin sections of AOs were rehydrated sequentially through ethanol and exposed to H&E to counterstain the nuclei and cytoplasm. Then, they were mounted with permount mounting medium (Fisher Scientific). Sirius red staining (ab150681; Abcam) were performed according to the manufacturers' instructions.

Statistical analysis

Statistical analyses and graphical presentation were performed using GraphPad Prism 9.0. All results are presented as the means and SDs of at least three independent experiments unless otherwise stated in the figure legends. Each error bar represents the SDs. Comparisons between two groups were analyzed using Student's t-test. Experiments involving three or more groups were analyzed by one-way or two-way ANOVA followed by Tukey's *post hoc* test. p-values <0.05 were regarded as statistically significant.

Results

Generation of *USP11* gene knockout in hiPSCs by CRISPR/Cas9

To gain further insights into the role of USP11 in the

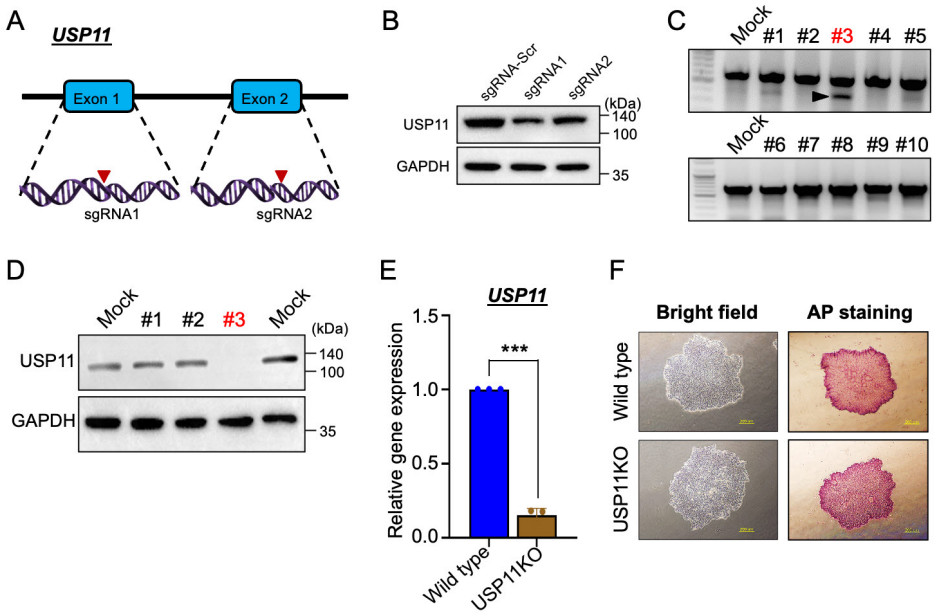

Fig. 1. Generation of *USP11* gene disruption in human induced pluripotent stem cells (hiPSCs). (A) The location of designed sgRNAs targeting *USP11* gene. (B) The efficiency of sgRNAs targeting USP11 was validated by western blot using the USP11 antibody. (C) The USP11 knockout clone in hiPSCs cell line was screened by T7 endonuclease 1 (T7E1) assay. The T7E1 positive clones showing cleavage are represented in red color. The arrowhead indicates the cleaved bands of the polymerase chain reaction (PCR) amplicons. (D) Western blot analysis showing USP11 knockout efficiency in hiPSCs cells. (E, F) The hiPSC-wildtype and hiPSC-USP11KO clones were characterized by (E) quantitative real-time reverse transcription-PCR using *USP11* gene primers and (F) AP staining, Scale bar=200 μm. Data are presented as the mean and SD of three independent experiments (n=3). Two-way ANOVA followed by Tukey's *post hoc* test was used to analyze. ***p<0.001.

progression of PF, we utilized the CRISPR/Cas9-mediated genome editing tool to knockout *USP11* gene in hiPSCs. To this end, we designed two individual sgRNAs that specifically targeted the *USP11* locus (Fig. 1A). The sgRNA1 showed higher reduction of USP11 expression than the sgRNA2 (Fig. 1B). Therefore, sgRNA1 was used along with Cas9-GFP for the transfection into hiPSCs. GFP-expressing Cas9-transfected hiPSCs were sorted using flow cytometry, and cells were expanded by seeding onto 96-well plates. *USP11* gene knockout single cell–derived mutant clones were screened by T7E1 assay (Fig. 1C). Western blot analysis showed that USP11 expression was abolished in clone #3 (hereafter hiPSC-USP11KO) (Fig. 1D). The quantitative real-time reverse transcription (qRT)-PCR result showed a complete reduction of USP11 mRNA level in hiPSC-USP11KO (Fig. 1E). Alkaline phosphatase staining (Fig. 1F), qRT-PCR analysis (Fig. 2A), Western blot analysis (Fig. 2B), and immunostaining analysis (Fig. 2C) for pluripotency markers showed similar expression levels of these markers in the hiPSC-USP11KO and wild- type hiPSCs, suggesting that the pluripotency status of the hiPSC-USP11KO was not altered by CRISPR/Cas9-mediated genome editing.

Differentiation of hiPSCs-USP11KO into AECs to generate AOs

We sought to differentiate hiPSCs-USP11KO into AECs to generate AOs. We followed our previously published optimized stepwise differentiation protocol to differentiate hiPSCs to AOs (9-11). We acquired distinct functional AECs, which were subsequently incubated in AEC maturation medium to generate AOs. Following a 30-day culture period, AOs were subjected to characterization studies. AOs generated from both hiPSC-wildtype and hiPSC-USP11KO exhibited a normal morphological behavior as shown by H&E staining (Fig. 2D). Interestingly, AOs derived from hiPSCs-USP11KO showed reduced expression of alveolar type 2 markers (*SFTPC* and *ABCA3*) and alveolar epithelial progenitor marker *NKX2.1* along with *USP11* expression (Fig. 2E) compared with AOs derived from hiPSC-wildtype, suggesting AEC2 abnormalities in hiPSCs-USP11KO-AOs.

TGF-β-mediated induction of PF in AOs

Next, we wished to investigate the role of USP11 in the progression of PF in AOs. To this end, we initially measured the effects of two fibrosis-inducing chemical agents, TGF-β and bleomycin (BLM), on AOs derived from

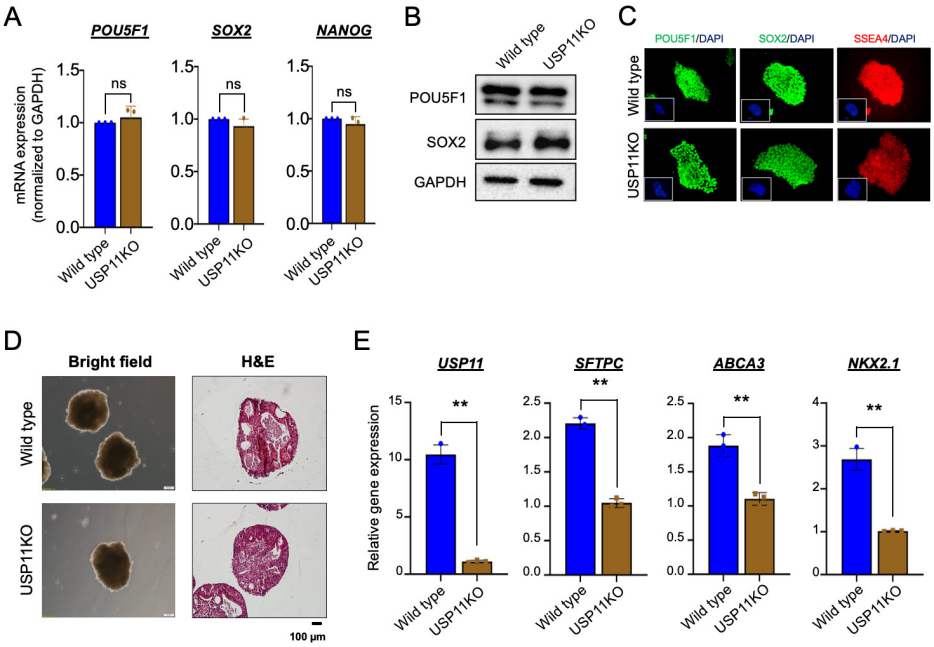

Fig. 2. Characterization of hiPSCs-USP11KO-AOs. (A) Quantitative real-time reverse transcription polymerase chain reaction (qRT-PCR) analysis using *POU5F1, SOX2,* and *NANOG* gene primers. (B) Western blot using POU5F1 and SOX2. (C) Immunostaining using the pluripotency markers POU5F1, SOX2, and SSEA4. Magnification: 100 μm. (D) The morphology of alveolar organoids (AOs) was analyzed by bright field and H&E staining. Scale bar=100 μm. (E) qRT-PCR analysis of AT2 markers (*SFTPC* and *ABCA3*) and alveolar epithelial progenitor marker *NKX2.1* along with *USP11* expression. Data are presented as the mean and SD of three independent experiments (n=3). Two-way ANOVA followed by Tukey's *post hoc* test was used to analyze. **p<0.01.

hiPSC-wildtype. qRT-PCR analysis revealed that TGF-β treatment induced stronger expression of EMT markers than BLM treatment (Fig. 3A). TGF-β treated hiPSC-wildtype demonstrated elevated expression of the mesenchymal markers N-cadherin and vimentin, while expression of the epithelial marker was reduced (Fig. 3A). Subsequently, we optimized the duration of TGF-β treatment and found that a 72 hours treatment resulted in the greatest induction of EMT markers among the time points evaluated (Fig. 3B). TGF-β treatment for 72 hours on hiPSC-wildtype exhibited normal morphological behavior in AOs but induced the expression of fibrotic markers including α-SMA and COL1A1 by immunostaining (Fig. 3C). Likewise, the fibrotic markers *α-SMA* and *COL1A1* (Fig. 3D) and EMT markers N-cadherin and vimentin (Fig. 3E) were also elevated at the mRNA level in TGF-β-treated hiPSCs-WT-AOs.

Loss of USP11 reduces fibrosis caused by TGF-β in hiPSCs-USP11KO-derived AOs

Next, we sought to investigate the effect of loss of function of USP11 on the progression of PF in AOs. To this end, we analyzed fibrotic changes at both protein and transcript levels in AOs treated with TGF-β to induce fibrosis. The hiPSCs-USP11KO-AOs showed complete absence of USP11 expression and reduced Sirius red staining compared to hiPSCs-USP11WT-AOs, suggesting that loss of USP11 reduces collagen deposition (Fig. 4A). The immunostaining analysis showed that loss of USP11 in hiPSCs-USP11KO-AOs exhibited abolished expression of USP11 and consequently diminished expression of fibrosis markers such as α-SMA, COL1A1 along with mesenchymal marker vimentin (Fig. 4A). Furthermore, mRNA expression analysis of TGF-β-treated hiPSCs-USP11KO-AOs showed reduced levels of fibrotic markers (*Fibronectin* and *COL1A1*) (Fig. 4B) and the mesenchymal marker *N-cadherin* compared with the hiPSCs-USP11WT-AOs (Fig. 4C). In contrast, expression of the epithelial marker *E-cadherin* was increased in TGF-β-treated hiPSCs-USP11KO-AOs when compared with hiPSCs-USP11WT-AOs (Fig. 4C), suggesting that loss of USP11 mitigates TGF-β-induced fibrosis in AOs.

Discussion

Lung organoids exhibit a tissue-specific functional characteristic and replicate the attributes of the original organ. AOs have been widely utilized to simulate pulmonary ill-

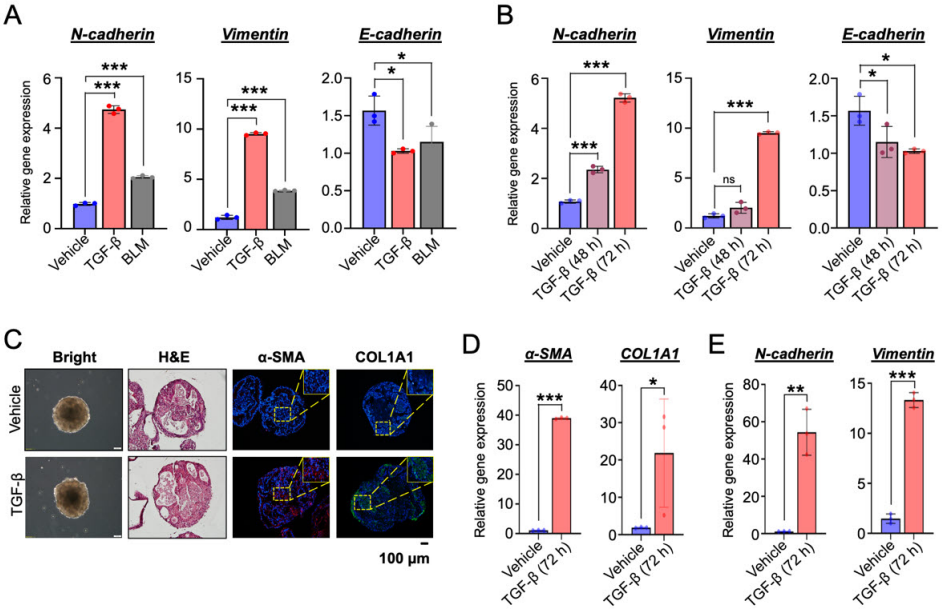

Fig. 3. Optimization of fibrosis induction by transforming growth factor (TGF)-β in human induced pluripotent stem cells-alveolar organoids (hiPSCs-AOs). (A) Comparison between TGF-β and bleomycin (BLM) chemicals for inducing fibrosis in hiPSC-AOs by quantitative real-time reverse transcription polymerase chain reaction (qRT-PCR) analysis using EMT markers (*N-cadherin, Vimentin*, and *E-cadherin*). (B) Optimum time duration for the induction of fibrosis by TGF-β in hiPSC-AOs was analyzed by qRT-PCR using EMT markers. (C, D) Characterization of fibrosis in hiPSC-AOs (C) by immunostaining using fibrotic markers (α-SMA and COL1A1) (scale bar=100 μm) and (D) qRT-PCR analysis using fibrotic marker gene primers (*α-SMA* and COL1A1). (E) qRT-PCR analysis using EMT marker (*N-cadherin* and *Vimentin*). Data are presented as the mean and SD of three independent experiments (n=3). Two-way ANOVA followed by Tukey's *post hoc* test was used to analyze. *$p<0.05$, **$p<0.01$, and ***$p<0.001$.

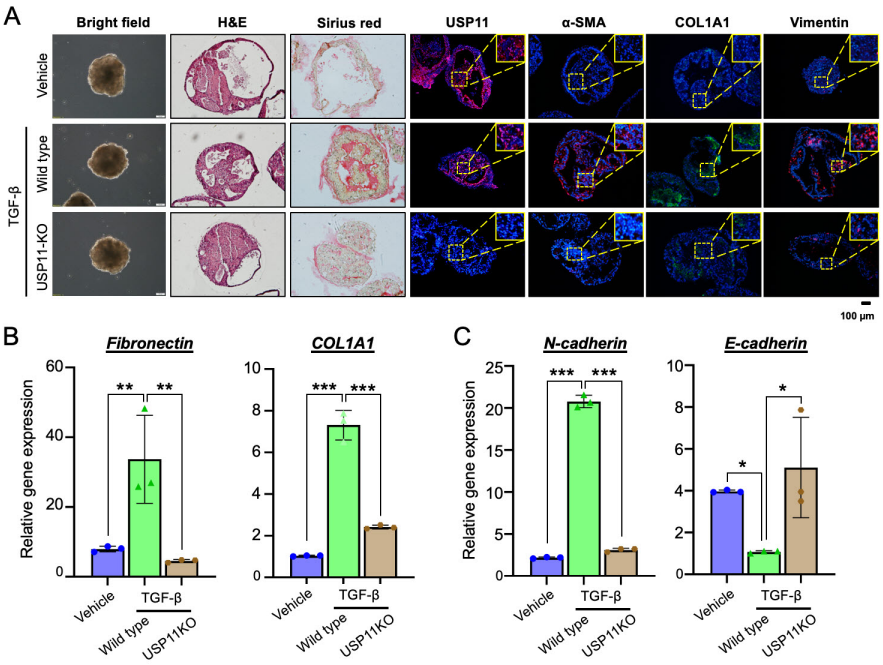

Fig. 4. The loss of USP11 mitigates pulmonary fibrosis (PF) in transforming growth factor (TGF)-β-induced PF in human induced pluripotent stem cells-alveolar organoids (hiPSCs-AOs). (A) The loss of function of USP11-mediated reduction of fibrosis in alveolar organoids was characterized by H&E staining, Sirius red staining and immunostaining with USP11, α-SMA, COL1A1, and Vimentin, scale bar=100 μm. (B) Quantitative real-time reverse transcription polymerase chain reaction (qRT-PCR) analysis of AOs using fibrosis markers *Fibronectin* and *COL1A1*. (C) qRT-PCR analysis of AOs using EMT markers *N-cadherin* and *E-cadherin*. Data are presented as the mean and SD of three independent experiments (n=3). Two-way ANOVA followed by Tukey's *post hoc* test was used to analyze. *p<0.05, **p<0.01, and ***p<0.001.

nesses and investigate their progression. The shape, polarity, rate of proliferation, gene expression, and genomic profile of the cells are all reflected in AOs. These AOs can also be utilized for drug screening, development of customized therapies, and investigation of the effectiveness of lung rehabilitation therapies.

USP11, a DUB that belongs to the USP family located in the X chromosome is known to interact with and deubiquitinate several proteins (12). USP11 regulates several biological functions such as DNA damage repair, viral RNA replication, and cell cycle progression (13-16). Recently, USP11 was known to promote profibrogenic and proinflammatory factors in uric acid-stimulated tubular epithelial cells and regulate the EMT process. However, the deletion of USP11 induced an anti-fibrotic and anti-inflammatory effect in *in vivo* models (17).

TGFβ-1 is regarded as the primary risk factor in lung fibrosis, with elevated levels of TGF-β being closely linked to the advancement of the lung fibrosis (18). Interestingly, USP11 was reported to be involved in TGF-β signaling by stabilizing TGF-β receptors TβRI and TβRII (8, 14). Considering that the expression of USP11 was elevated in human IPF patient samples (19), we sought to investigate the effect of loss of USP11 function in the development of PF in AOs. No studies have investigated the involvement of USP11 in the progression of PF during differentiation of human embryonic stem cells into lung tissue. Thus, we employed the CRISPR/Cas9 system to knock out the *USP11* gene in hiPSCs, and then differentiated these knockout cells into AOs and treated the AOs with TGF-β to induce PF. TGF-β induces the overproduction of extracellular matrix proteins, resulting in lung scarring and hardening (20). Functional impairment of USP11 decreased collagen deposition and expression of fibrotic markers at both protein and mRNA levels (Fig. 4). Altogether, our results demonstrate that USP11 might be a potential therapeutic target to mitigate PF in IPF patients.

ORCID

Sripriya Rajkumar, https://orcid.org/0009-0006-4336-130X
Ji-Hye Jung, https://orcid.org/0000-0003-1638-8823
Ji-Young Kim, https://orcid.org/0000-0002-0112-2603
Janardhan Keshav Karapurkar, https://orcid.org/0000-0002-0198-4035
Girish Birappa, https://orcid.org/0009-0000-7145-3638
D. A. Ayush Gowda, https://orcid.org/0009-0001-7819-5456
C. Bindu Ajaykumar, https://orcid.org/0009-0001-2937-1046

Haribalan Perumalsamy, https://orcid.org/0000-0002-6497-5857
Bharathi Suresh, https://orcid.org/0009-0005-3277-9455
Kye-Seong Kim, https://orcid.org/0000-0001-5550-1660
Seok-Ho Hong, https://orcid.org/0000-0003-3372-442X
Suresh Ramakrishna, https://orcid.org/0000-0002-4038-1085

Funding

This research was also supported by the Bio & Medical Technology Development Program of the National Research Foundation (NRF) funded by the Korean government (MSIT) (RS-2022-NR067319) and NRF of Korea (RS-2023-00279214 and RS-2024-00341469).

Potential Conflict of Interest

There is no potential conflict of interest to declare.

Authors' Contribution

Conceptualization: Sripriya Rajkumar, JHJ, JYK, SHH. Data curation: Sripriya Rajkumar, JHJ, JYK. Formal analysis: Sripriya Rajkumar, JHJ, JYK, Suresh Ramakrishna, SHH. Funding acquisition: KSK, SHH, Suresh Ramakrishna. Investigation: Sripriya Rajkumar, JHJ. Methodology: JYK, JKK, GB, DAAG, CBA, HP, BS. Project administration: KSK, SHH, Suresh Ramakrishna. Resources: KSK, SHH, Suresh Ramakrishna. Software: HP. Supervision: KSK, SHH, Suresh Ramakrishna. Validation: Sripriya Rajkumar, JHJ, JYK. Visualization: Sripriya Rajkumar, JHJ, JYK. Writing – original draft: Sripriya Rajkumar, JHJ, JYK. Writing – review and editing: KSK, SHH, Suresh Ramakrishna.

Supplementary Materials

Supplementary data including four tables can be found with this article online at https://doi.org/10.15283/ijsc25011

References

1. Blokland KEC, Waters DW, Schuliga M, et al. Senescence of IPF lung fibroblasts disrupt alveolar epithelial cell proliferation and promote migration in wound healing. Pharmaceutics 2020;12:389
2. Confalonieri P, Volpe MC, Jacob J, et al. Regeneration or repair? The role of alveolar epithelial cells in the pathogenesis of idiopathic pulmonary fibrosis (IPF). Cells 2022;11:2095
3. Salton F, Ruaro B, Confalonieri P, Confalonieri M. Epithelial-mesenchymal transition: a major pathogenic driver in idiopathic pulmonary fibrosis? Medicina (Kaunas) 2020;56:608
4. Lederer DJ, Martinez FJ. Idiopathic pulmonary fibrosis. N Engl J Med 2018;378:1811-1823
5. Basu B, Ghosh MK. Ubiquitination and deubiquitination in the regulation of epithelial-mesenchymal transition in cancer: shifting gears at the molecular level. Biochim Biophys Acta Mol Cell Res 2022;1869:119261
6. Farshi P, Deshmukh RR, Nwankwo JO, et al. Deubiquitinases (DUBs) and DUB inhibitors: a patent review. Expert Opin Ther Pat 2015;25:1191-1208
7. Ge C, Huang M, Han Y, Shou C, Li D, Zhang Y. Demethyleneberberine alleviates pulmonary fibrosis through disruption of USP11 deubiquitinating GREM1. Pharmaceuticals (Basel) 2024;17:279
8. Jacko AM, Nan L, Li S, et al. De-ubiquitinating enzyme, USP11, promotes transforming growth factor β-1 signaling through stabilization of transforming growth factor β receptor II. Cell Death Dis 2016;7:e2474
9. Jacob A, Morley M, Hawkins F, et al. Differentiation of human pluripotent stem cells into functional lung alveolar epithelial cells. Cell Stem Cell 2017;21:472-488.e10
10. Jacob A, Vedaie M, Roberts DA, et al. Derivation of self-renewing lung alveolar epithelial type II cells from human pluripotent stem cells. Nat Protoc 2019;14:3303-3332
11. Kim JH, An GH, Kim JY, et al. Human pluripotent stem-cell-derived alveolar organoids for modeling pulmonary fibrosis and drug testing. Cell Death Discov 2021;7:48
12. Ideguchi H, Ueda A, Tanaka M, et al. Structural and functional characterization of the USP11 deubiquitinating enzyme, which interacts with the RanGTP-associated protein RanBPM. Biochem J 2002;367(Pt 1):87-95
13. Schoenfeld AR, Apgar S, Dolios G, Wang R, Aaronson SA. BRCA2 is ubiquitinated *in vivo* and interacts with USP11, a deubiquitinating enzyme that exhibits prosurvival function in the cellular response to DNA damage. Mol Cell Biol 2004;24:7444-7455
14. Al-Salihi MA, Herhaus L, Macartney T, Sapkota GP. USP11 augments TGFβ signalling by deubiquitylating ALK5. Open Biol 2012;2:120063
15. Wu HC, Lin YC, Liu CH, et al. USP11 regulates PML stability to control Notch-induced malignancy in brain tumours. Nat Commun 2014;5:3214
16. Yu M, Liu K, Mao Z, Luo J, Gu W, Zhao W. USP11 is a negative regulator to γH2AX ubiquitylation by RNF8/RNF168. J Biol Chem 2016;291:959-967.
17. Shi Y, Tao M, Chen H, et al. Ubiquitin-specific protease 11 promotes partial epithelial-to-mesenchymal transition by deubiquitinating the epidermal growth factor receptor during kidney fibrosis. Kidney Int 2023;103:544-564
18. Yue X, Shan B, Lasky JA. TGF-β: titan of lung fibrogenesis. Curr Enzym Inhib 2010;6:10.2174/10067
19. Tang Y, Yuan Q, Zhao C, et al. Targeting USP11 may alleviate radiation-induced pulmonary fibrosis by regulating endothelium tight junction. Int J Radiat Biol 2022;98:30-40
20. Frangogiannis N. Transforming growth factor-β in tissue fibrosis. J Exp Med 2020;217:e20190103